Biogeochemistry **48:** 91–114, 2000.

Modeling the effects of snowpack on heterotrophic respiration across northern temperate and high latitude regions: Comparison with measurements of atmospheric carbon dioxide in high latitudes

A.D. McGUIRE[1], J.M. MELILLO[2], J.T. RANDERSON[3], W.J. PARTON[4], M. HEIMANN[5], R.A. MEIER[6], J.S. CLEIN[6], D.W. KICKLIGHTER[2] & W. SAUF[5]
[1]*U.S. Geological Survey, Alaska Cooperative Fish and Wildlife Research Unit, University of Alaska Fairbanks, Fairbanks, AK, U.S.A.;* [2]*The Ecosystems Center, Marine Biological Laboratory, Woods Hole, MA, U.S.A.;* [3]*Center for Atmospheric Sciences, University of California, Berkeley, CA, U.S.A.;* [4]*Natural Resources Ecology Laboratory, Colorado State University, Fort Collins, CO, U.S.A.;* [5]*Max-Planck-Institut für Meteorologie, Hamburg, Germany;* [6]*Institute of Arctic Biology, University of Alaska Fairbanks, Fairbanks, AK, U.S.A.*

Received 10 February 1999; accepted 23 February 1999

Key words: carbon dioxide, ecological modeling, global carbon cycle, heterotrophic respiration, net ecosystem production

Abstract. Simulations by global terrestrial biogeochemical models (TBMs) consistently underestimate the concentration of atmospheric carbon dioxide (CO_2) at high latitude monitoring stations during the nongrowing season. We hypothesized that heterotrophic respiration is underestimated during the nongrowing season primarily because TBMs do not generally consider the insulative effects of snowpack on soil temperature. To evaluate this hypothesis, we compared the performance of baseline and modified versions of three TBMs in simulating the seasonal cycle of atmospheric CO_2 at high latitude CO_2 monitoring stations; the modified version maintained soil temperature at 0 °C when modeled snowpack was present. The three TBMs include the Carnegie-Ames-Stanford Approach (CASA), Century, and the Terrestrial Ecosystem Model (TEM). In comparison with the baseline simulation of each model, the snowpack simulations caused higher releases of CO_2 between November and March and greater uptake of CO_2 between June and August for latitudes north of 30° N. We coupled the monthly estimates of CO_2 exchange, the seasonal carbon dioxide flux fields generated by the HAMOCC3 seasonal ocean carbon cycle model, and fossil fuel source fields derived from standard sources to the three-dimensional atmospheric transport model TM2 forced by observed winds to simulate the seasonal cycle of atmospheric CO_2 at each of seven high latitude monitoring stations. In comparison to the CO_2 concentrations simulated with the baseline fluxes of each TBM, concentrations simulated using the snowpack fluxes are generally in better agreement with observed concentrations between August and March at each of the monitoring stations. Thus, representation of the insulative effects of snowpack in TBMs generally improves simulation of atmospheric CO_2 concentrations in high latitudes during both the late growing season and nongrowing season. These simulations highlight the global importance of biogeochemical processes during the nongrowing season in estimating carbon balance of ecosystems in northern high and temperate latitudes.

Introduction

There is evidence that warming is occurring in some high-latitude areas (Lachenbruch & Marshall 1986; Beltrami & Mareschal 1991; Chapman & Walsh 1993), and that the warming may be impacting both ecosystem function and structure (Oechel et al. 1993, 1995; Chapin et al. 1995). These ecosystems contain approximately 40% of the world's soil carbon inventory that is potentially reactive in the context of near-term climate change (McGuire et al. 1995; Melillo et al. 1995; McGuire & Hobbie 1997). A substantial amount of carbon could be released in inorganic forms from these soils in response to elevated temperature (Nadelhoffer et al. 1992; Oechel et al. 1993, 1995). A large release of CO_2 from these soils has the potential to influence the growth of atmospheric CO_2, which may have consequences for the rate and magnitude of climate change.

During the late 1980's, substantial releases of CO_2 were observed from Alaskan tundra ecosystems in response to declining water tables associated with elevated temperature (Oechel et al. 1993). Recent measurements of CO_2 exchange between tundra ecosystems and the atmosphere indicate that substantial losses of CO_2 from tundra soils may occur during the fall, winter, and spring months (Zimov et al. 1993, 1996; Oechel et al. 1997). Recent measurements at some locations indicate that these losses are currently greater than sink activity in summer months (Oechel and Vourlitis, unpublished). Thus, estimates of carbon balance in high latitude ecosystems are potentially biased if they are based on summer measurements alone (Oechel et al. 1997).

A number of global terrestrial biogeochemical models (TBMs) have been developed to assess the effects of changes in climate and atmospheric carbon dioxide on terrestrial ecosystem processes at large spatial scales (Heimann et al. 1998; Cramer et al. 1999; Kicklighter et al. 1999). For typical global application, TBMs make estimates of monthly CO_2 exchanges between terrestrial ecosystems and the atmosphere for approximately 60,000 grid cells at a spatial resolution of 0.5° by 0.5° (latitude by longitude), with about one-third of these estimates in high latitudes. Heimann et al. (1998) compared the performance of several TBMs by using the monthly estimates of CO_2 exchange by the models to simulate the seasonal cycle of atmospheric CO_2 at a number of CO_2 monitoring stations located throughout the globe. At high latitude monitoring stations, the simulations consistently underestimated the concentration of atmospheric CO_2 during the nongrowing season, which suggests that global TBMs tend to underestimate the release of CO_2 from high latitude soils during the nongrowing season. We hypothesize that decomposition is underestimated during the nongrowing season primarily because the TBMs do not consider the insulative effects of snow on soil temperature. In this study we modify the decomposition formulation of three TBMs to evaluate whether consideration of the insulative effects of snowpack improves the simulation of monthly concentrations of atmospheric CO_2 at CO_2 monitoring stations located in high latitudes.

Modeling the seasonal cycle of atmospheric CO_2

Overview

To model the seasonal cycle of atmospheric CO_2 at a monitoring station requires spatially explicit seasonal estimates of carbon exchange between the atmosphere, the oceans, and the terrestrial surface (Figure 1). In the absence of disturbance and major climatic fluctuations, annual net primary production (NPP) and annual heterotrophic respiration (R_H; i.e., decomposition) of terrestrial ecosystems are approximately in balance. Because photosynthesis and microbial activity are controlled in different ways by environmental and biotic factors, the magnitudes of NPP and R_H are not synchronized throughout the year. Here we adopt the ecological convention that fluxes into the land surface are positive. On a monthly basis, net ecosystem production (NEP), which is the difference between monthly NPP and R_H, can either be positive or negative; positive values indicate sink activity and negative values represent source activity. The seasonal fluctuations of NEP are primarily responsible for the observed seasonal variation in the concentration of atmospheric CO_2, especially at high northern latitudes where these variations have the greatest amplitude (Fung et al. 1983, 1987; Heimann et al. 1989, 1998).

In this study we conducted two simulations with each of three TBMs to evaluate how a representation of the insulative effects of snowpack influences the seasonal cycle of atmospheric CO_2 at high latitude monitoring stations in comparison to the baseline version of each model. For the snowpack version of each model, we modified the R_H formulation in the baseline version so that temperature is maintained at 0 °C when modeled snowpack is present. For each simulation in this study, monthly NPP, R_H, and NEP are estimated for each 0.5° grid cell of the terrestrial biosphere. The spatially explicit monthly NEP estimates are combined with equivalent CO_2 flux fields generated by an ocean biogeochemical model, and fossil fuel source fields; monthly CO_2 emission fields from fossil fuel burning and cement manufac-

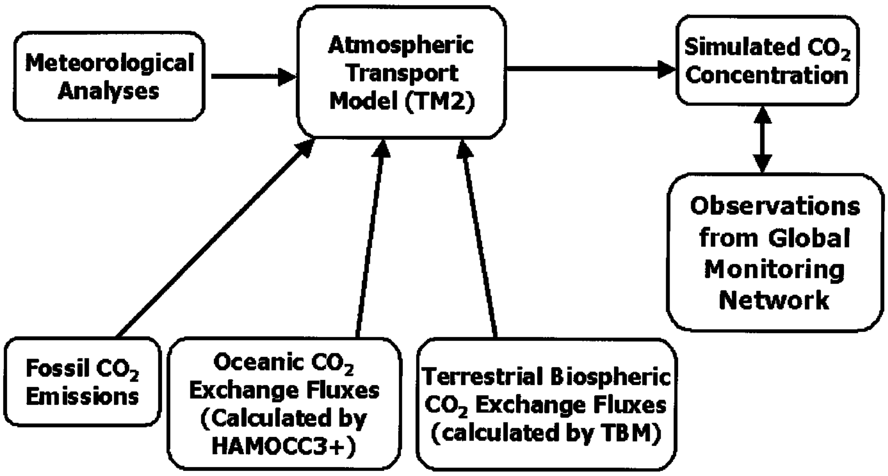

Figure 1. Flowchart of the data flow and model linkages for simulating the seasonal cycle of atmospheric CO_2.

ture are computed based on a global 1° × 1° map compiled by Marland et al. (1989) assuming constant emissions throughout the year. The terrestrial, oceanic, and fossil fuel fields of CO_2 fluxes provide the lower boundary condition for a three-dimensional atmospheric transport model forced by observed winds. To evaluate the simulation of atmospheric CO_2 concentrations, we extracted the monthly estimates of atmospheric CO_2 from locations corresponding to monitoring stations and compared the estimates with the detrended observations at each station.

In a previous study (Heimann et al. 1998), we obtained observed atmospheric CO_2 concentrations for the years 1983–1992 from the monitoring program of the National Oceanographic and Atmospheric Administration (NOAA; Conway et al. 1994a, 1994b). The seasonal cycle of atmospheric CO_2 was extracted from the raw station data at 27 monitoring stations, as described by Heimann et al. (1998). Among the 27 stations, we focus our comparison between simulated and observed concentrations of atmospheric CO_2 on the seven most northern stations (Table 1). Because these stations effectively integrate seasonal CO_2 exchanges across much of the northern hemisphere (Kaminski et al. 1996), we focus our evaluation of the seasonal patterns of CO_2 exchange on northern high latitudes between 60° N and 90° N and on northern temperate latitudes between 30° N and 60° N. To evaluate how well a simulation reproduces the observed seasonal signal of atmospheric CO_2 at a monitoring station, we calculated a normalized mean-squared deviation (NMSD) as

Table 1. Stations from the NOAA station network (Conway et al. 1994b) used in this study.

#	Abbreviation	Station	Country	Latitude	Longitude	Elevation [m]
1	ALT	Alert, N.W.T.	Canada	82°27′ N	62°31′ W	210
2	MBC	Mould Bay, N.W.T.	Canada	76°14’N	119°20′ W	15
3	KTL	Kotelny Island, Siberia	Russia	76°06′ N	137°36′ E	5
4	BRW	Point Barrow, Alaska	U.S.	71°19′ N	156°36′ W	11
5	STM	Ocean Station “M”	Norway	66°00′ N	2°00′ E	6
6	CBA	Cold Bay, Alaska	U.S.	55°12′ N	162°43′W	25
7	SHM	Shemya Island	U.S.	52°43′ N	174°06′ E	40

$$\mathrm{NMSD} = \frac{1}{12} \cdot \sum_{\mathrm{m}=1}^{12} \left(\frac{([\mathrm{TBM}]_\mathrm{m} + [\mathrm{FOS}]_\mathrm{m} + [\mathrm{OCE}]_\mathrm{m} - [\mathrm{OBS}_\mathrm{m}])^2}{\sigma_\mathrm{m}^2} \right),$$

where $[\mathrm{TBM}]_\mathrm{m}$, $[\mathrm{FOS}]_\mathrm{m}$, and $[\mathrm{OCE}]_\mathrm{m}$ are the monthly CO_2 concentrations resulting from the corresponding biospheric, fossil fuel, and ocean flux, respectively, $[\mathrm{OBS}]_\mathrm{m}$ is the mean observed value of CO_2 (from available data in the 1983 to 1992 period) and σ_m is the standard deviation of the observed value for each month (m = 1, 2, . . . 12) of the year.

In this study we used the HAMOCC3 ocean biogeochemical model (Maier-Reimer 1993; Six & Maier-Reimer 1996) and the TM2 atmospheric transport model (Heimann 1995). The description and application of these models for purposes of simulating the seasonal cycle of atmospheric CO_2 is documented in Heimann et al. (1998). The three TBMs we applied in this study include the Carnegie-Ames-Stanford Approach (CASA; Randerson et al. 1997), Century (Parton et al. 1993), and the Terrestrial Ecosystem Model (TEM; McGuire et al. 1997; Tian et al. 1999). The data sets used as driving variables for each model are the same as used in the “Potsdam 95” comparison of NPP among global TBMs (Cramer et al. 1999), a comparison which included the three TBMs in this study. Differences in the absolute magnitude of global and regional NPP among the three TBMs have been described in Cramer et al. (1999) and Kicklighter et al. (1999). One important difference among the models concerns controls over the phenology of NPP. In CASA, the phenology of NPP is largely determined from satellite-derived data. In contrast, Century and TEM implement prognostic phenology algorithms. To facilitate evaluation of the seasonality of NPP and R_H among the models in this study, we focus our comparison on the relative proportion of annual NPP and annual R_H that is estimated to occur in each month of the year within northern high and temperate latitudes. In the following sections we provide additional details on the description of the TBMs.

The Carnegie-Ames-Stanford Approach (CASA)

The CASA model calculates NPP from satellite-derived photosynthetically active radiation using a light use efficiency model (Field et al. 1995, 1998). For each monthly time step, a globally uniform maximum light use efficiency (ε^*) is reduced by temperature and soil moisture stress scalars that reflect local environmental conditions. The calibration process involves adjusting ε^* to minimize the difference between observed and modeled NPP estimates across a number of sites worldwide. Simulated NPP in CASA is allocated to three living biomass pools, which include leaves, fine roots, and wood (Thompson et al. 1996).

Biomass is delivered to the soil as leaf litterfall, coarse woody debris, and fine root turnover (Randerson et al. 1996). Transformations of soil organic matter are represented following the structure of the Century model, with a suite of active and slow organic matter fractions (Parton et al. 1993). In the version of CASA used in this study, the ratio of carbon to nitrogen in leaf litterfall is held constant for each biome type (Randerson et al. 1996). A Q_{10} of 1.5 is used to describe the response of microbial activity to surface air temperature (Raich & Potter 1995).

Century

The Century model uses information on climate, atmospheric CO_2, and nitrogen inputs to estimate the monthly fluxes and pools of carbon and nitrogen in terrestrial ecosystems (Parton et al. 1987, 1993). In this study, we applied version 4.0 of Century, which is described by Parton et al. (1993). In Century, maximum plant production is controlled by soil temperature, available water, and leaf area. A temperature-production function is specified according to plant functional types, such as C_3 cool season plants or C_4 warm season plants. Production is further modified by the current amount of aboveground plant material (i.e., self-shading), atmospheric CO_2 concentrations, and available soil nitrogen. To simulate savanna and shrubland ecosystems, grass and forest components compete for water, light, and nutrients in a prescribed manner. Simulated NPP in Century is allocated to eight vegetation pools.

Tissues that senescence from the vegetation pools of Century enter the soil as plant residues. The Century model simulates the decomposition of plant residues with a detailed submodel (13 pools) that divides soil organic carbon into three fractions: an active soil fraction ($<$10-year turnover time) consisting of live microbes and microbial products; a protected fraction (decadal turnover time) that is more resistant to decomposition as a result of physical or chemical protection; and a fraction that has a very long turnover time (millenial turnover time). The decomposition of each soil organic fraction is calculated at a monthly time step as a function of the soil organic carbon in the fraction, air temperature, and soil moisture. A Q_{10} of approximately 1.6 is used to describe the response of microbial activity to surface air temperature.

The Terrestrial Ecosystem Model (TEM)

The TEM is a highly aggregated TBM that uses spatially referenced information on climate, elevation, soils, and vegetation to make monthly estimates of important carbon and nitrogen fluxes and pool sizes in the global terrestrial biosphere. In this study we applied version 4.1 of TEM, in which the formulations for autotrophic and heterotrophic respiration have been modified from earlier versions as described in McGuire et al. (1997) and Tian et al. (1999). In TEM, NPP is the difference between carbon captured from the atmosphere as gross primary production (GPP) and carbon respired to the atmosphere by the vegetation. Monthly GPP is initially calculated in TEM as a function of photosynthetically active radiation, air temperature, atmospheric carbon dioxide concentration, and moisture availability. If nitrogen supply, which is the sum of nitrogen uptake and labile nitrogen in the vegetation, cannot meet the stoichiometric carbon to nitrogen ratio of biomass production, then GPP is reduced to meet the constraint. In the case where nitrogen supply does not limit biomass production, nitrogen uptake is reduced so that nitrogen supply meets the constraint of biomass production. In this way, the carbon-nitrogen status of the vegetation causes the model to allocate more effort toward either carbon or nitrogen uptake (McGuire et al. 1992). Plant respiration, which includes growth and maintenance respiration, is a function of GPP, vegetation carbon, and surface air temperature.

Biomass is delivered to the soil as litter production, which is calculated as a linear function of vegetation carbon (Raich et al. 1991). In TEM, the flux R_H represents decomposition of all organic matter in an ecosystem and is calculated at a monthly time step as a function of one soil organic carbon compartment, air temperature, and soil moisture. Although the model does not track separate pools of soil organic matter, the formulations in the model implicitly consider issues of organic matter quality and turnover (McGuire et al. 1995, 1997). A Q_{10} of 2.0 is used to describe the response of microbial activity to surface air temperature (Raich et al. 1991).

Results

For northern high latitudes, the baseline simulations of all three models estimate that monthly NPP is positive between May and September, with very low or negative values estimated during other months of the year (Figure 2(a–c)). The CASA baseline simulation estimates that approximately 40% of annual NPP in northern high latitudes occurs in July, with June and August as the next two most productive months. In contrast, both the Century and TEM baseline simulations estimate that maximum production occurs in June, with July and August as the next two most productive months. For all three models, implementation of the snowpack formulation has little effect on the proportion of annual NPP that is estimated to occur in each month.

In the baseline simulations of all three models, positive values of monthly R_H are estimated for each month of the year for northern high latitudes, with the lowest monthly estimates in December and January and the highest estimates in July (Figure 2(d–f)). Although minimum and maximum R_H of the snowpack simulations of the three models tends to occur in the same months as in the baseline simulations, the proportion of annual R_H estimated by the snowpack simulations is lower between May and September and higher between November and March.

For northern temperate latitudes, the baseline simulation of all three models estimate positive values of NPP between February and November (Figure 3(a–c)). For December and January, the CASA and Century baseline simulations estimate low positive NPP while the TEM baseline simulation estimates low negative NPP. The baseline simulation of CASA estimates that July is the most productive month in northern temperate latitudes with June and August being the next two most productive months. In contrast, the baseline simulations of Century and TEM estimate that maximum production occurs in May and June, respectively. Similar to northern high latitudes, implementation of the snowpack formulation in each model has little effect on the proportion of annual NPP that is estimated to occur in each month.

Similar to northern high latitudes, positive values of monthly R_H are estimated for each month of the year for northern temperate latitudes by the baseline simulation of each model, with the lowest monthly estimates in December and January and the highest estimates in July (Figure 3(d–f)). Although minimum and maximum R_H of the snowpack simulations of the three models tends to occur in the same months as in the baseline simulations, the proportion of annual R_H estimated by the snowpack simulations is lower between April and October and higher between November and March.

The differences in the monthly proportions of annual R_H between the baseline and snowpack simulations cause differences in the seasonal uptake and release of CO_2 between the two simulations of all three models in

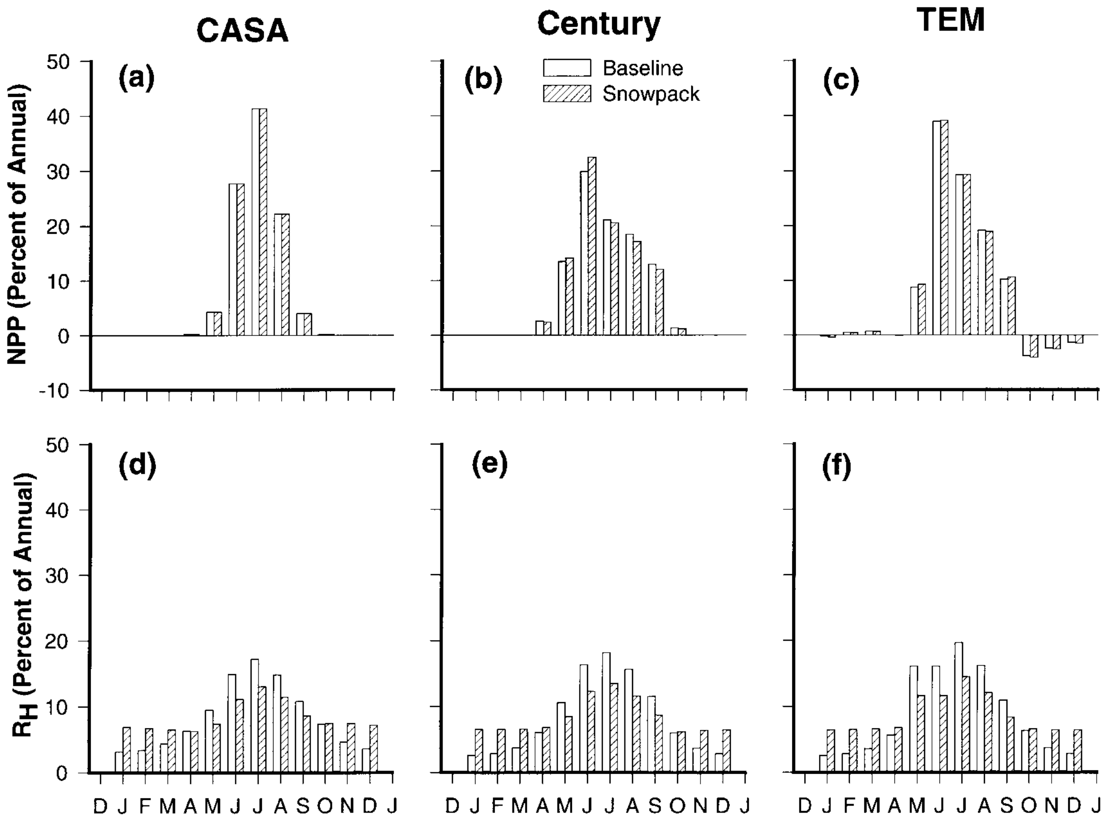

Figure 2. Relative proportions of annual net primary production (NPP) and heterotrophic respiration (R_H) that occur during each month of the year for baseline simulations (open bars) and snowpack simulations (hatched bars) between 60° N and 90° N for (a, d) the Carnegie-Ames-Stanford Approach (CASA), (b, e) Century, and (c, f) the Terrestrial Ecosystem Model (TEM).

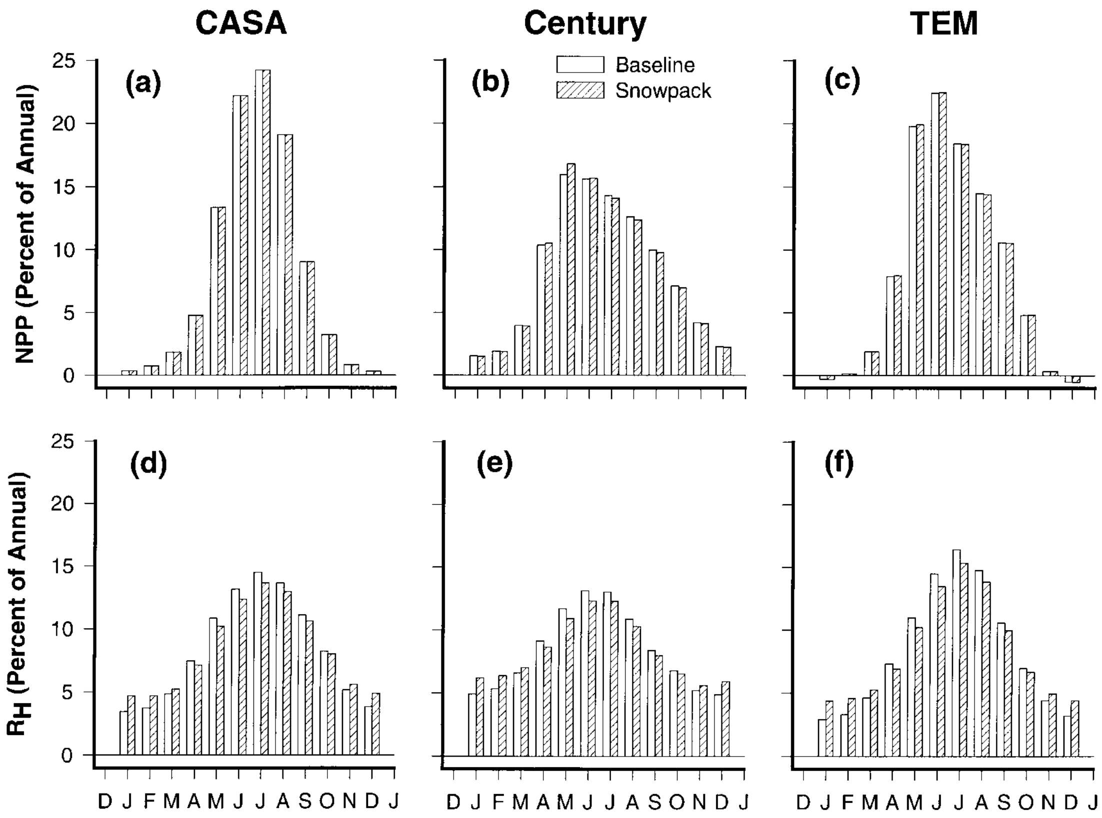

Figure 3. Relative proportions of annual net primary production (NPP) and heterotrophic respiration (R_H) that occur during each month of the year for baseline simulations (open bars) and snowpack simulations (hatched bars) between 30° N and 60° N for (a, d) the Carnegie-Ames-Stanford Approach (CASA), (b, e) Century, and (c, f) the Terrestrial Ecosystem Model (TEM).

both northern high latitudes and northern temperate latitudes. For northern high latitudes, the snowpack simulations of all three models estimate greater uptake between June and August and greater release between November and March in comparison to the baseline simulations (Figure 4(a–c)). For comparison with Oechel et al. (1997), we analyzed the releases of CO_2 estimated for each of the models between October and May in northern high latitudes. Between October and May, the snowpack simulations estimate that the release of CO_2 from high latitude soils is 1241 10^{12} g C (Tg C) for CASA, 543 Tg C for Century, and 1219 Tg C for TEM, which is 36%, 124%, and 41% higher than the estimates in the baseline simulations, respectively. Specifically in wet/moist tundra, the release of CO_2 estimated between October and May by the snowpack simulations is 112 g C m^{-2} for CASA, 50 g C m^{-2} for Century, and 62 g C m^{-2} for TEM. Similar to northern high latitudes, the snowpack simulations of all three models estimate greater uptake between May and August and greater release between November and March in northern temperate latitudes (Figure 4(c–e)). In comparison to the baseline simulations, the greater uptake of CO_2 from the atmosphere during the growing season and the greater release CO_2 to the atmosphere during the nongrowing season estimated by the snowpack simulations for terrestrial ecosystems north of 30° N has implications for the simulation of the seasonal cycle of atmospheric CO_2 at high latitude monitoring stations.

In comparison to the CO_2 concentrations simulated with the baseline fluxes of each biogeochemical model, the CO_2 concentrations simulated using the snowpack fluxes are generally in better agreement with observed concentrations between August and March at each of seven monitoring stations located in northern high latitudes (Figures 5, 6, and 7). There appears to be little effect of the snowpack simulations on the CO_2 concentrations simulated for May, June, and July. Among the seven high latitude stations, the normalized mean squared deviation between estimated and observed CO_2 concentrations was significantly improved for CO_2 fluxes associated with the snowpack simulation of each terrestrial biosphere model (Figure 8; for each TBM, Wilcoxin-signed rank test: $W = -28.0$, $P = 0.016$, $N = 7$). Thus, representation of the insulative effects of snowpack in TBMs generally improves simulation of atmospheric CO_2 concentrations in high latitudes during both the late growing season and the nongrowing season, and has little effect on concentrations at the beginning of the growing season.

Discussion

The observation that heterotrophic respiration during the nongrowing season represents a substantial proportion of annual heterotrophic respiration has

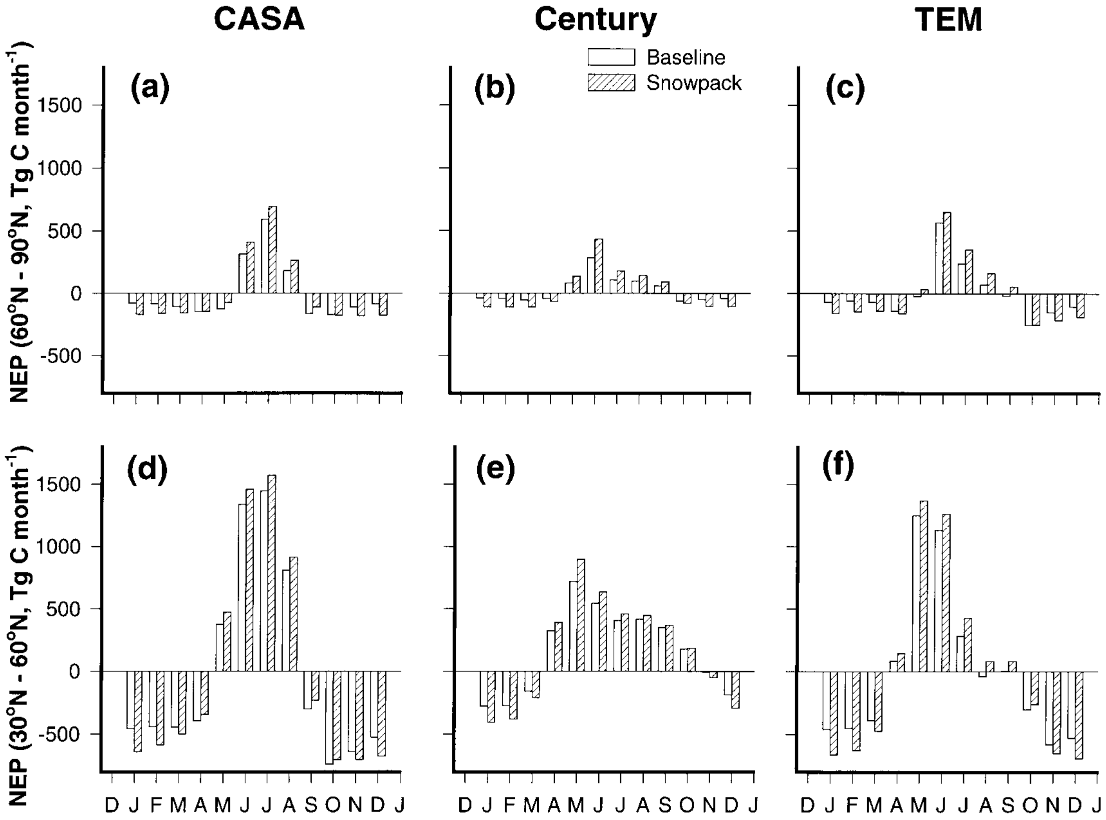

Figure 4. Monthly net ecosystem production (NEP) for baseline simulations (open bars) and snowpack simulations (hatched bars) from (a, b, c) 60° N to 90° N and (d, e, f) 30° N to 60° N for the Carnegie-Ames-Stanford Approach (CASA), Century, and the Terrestrial Ecosystem Model (TEM).

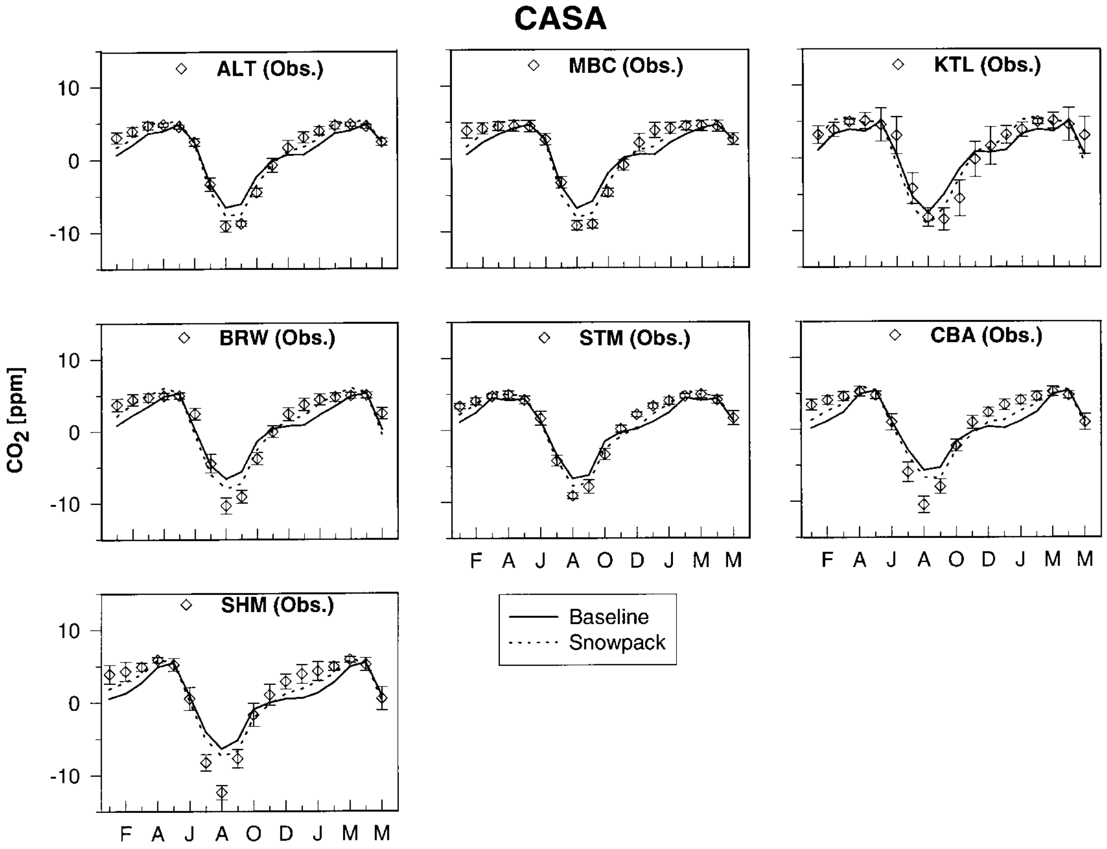

Figure 5. Comparison between the observed seasonal cycle of CO_2 and the simulated seasonal cycle produced by coupling the monthly estimates of net ecosystem production estimated by the Carnegie-Ames-Stanford Approach (CASA) and fossil fuel emissions with the Hamburg ocean and atmospheric transport models for each of the seven high latitude monitoring stations. The first six months of each cycle are displayed twice to reveal the annual variation more clearly. Mean and standard deviation are shown for the observed data. Station abbreviations are identified in Table 1.

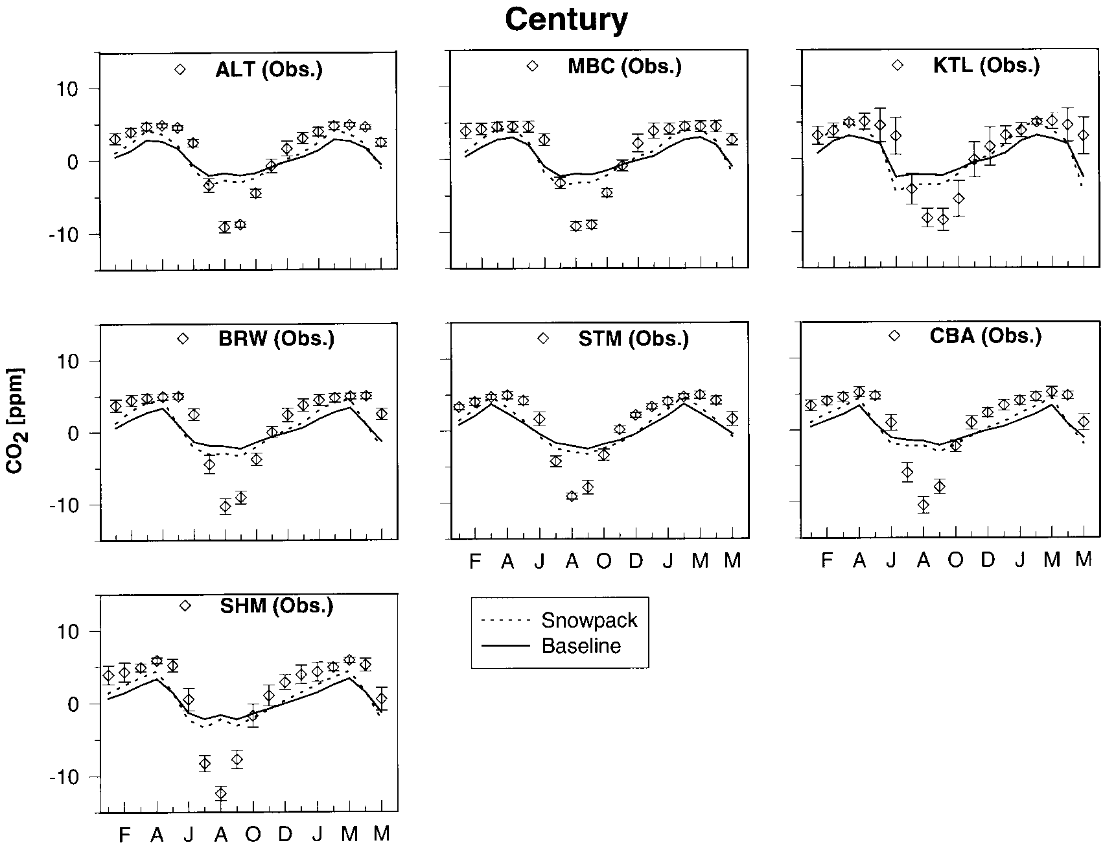

Figure 6. Comparison between the observed seasonal cycle of CO_2 and the simulated seasonal cycle produced by coupling the monthly estimates of net ecosystem production estimated by the Century model and fossil fuel emissions with the Hamburg ocean and atmospheric transport models for each of the seven high latitude monitoring stations. The first six months of each cycle are displayed twice to reveal the annual variation more clearly. Mean and standard deviation are shown for the observed data. Station abbreviations are identified in Table 1.

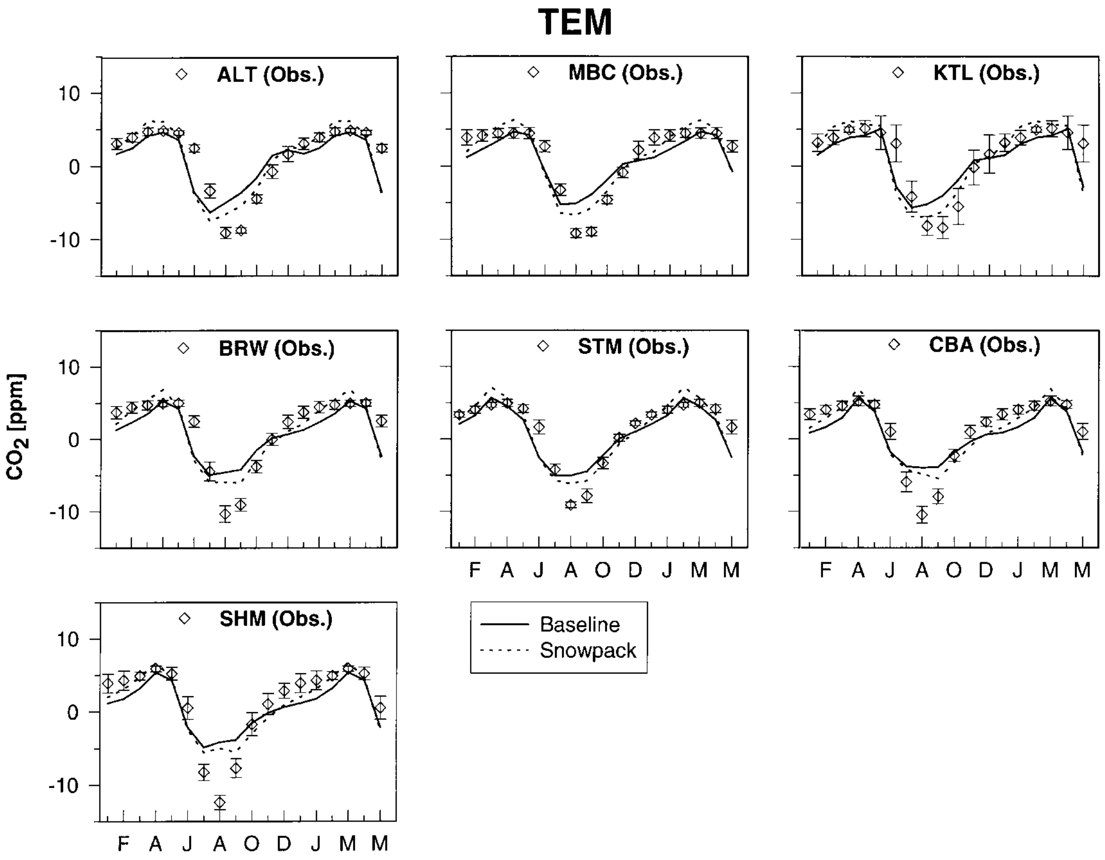

Figure 7. Comparison between the observed seasonal cycle of CO_2 and the simulated seasonal cycle produced by coupling the monthly estimates of net ecosystem production estimated by the Terrestrial Ecosystem Model (TEM) and fossil fuel emissions with the Hamburg ocean and atmospheric transport models for each of the seven high latitude monitoring stations. The first six months of each cycle are displayed twice to reveal the annual variation more clearly. Mean and standard deviation are shown for the observed data. Station abbreviations are identified in Table 1.

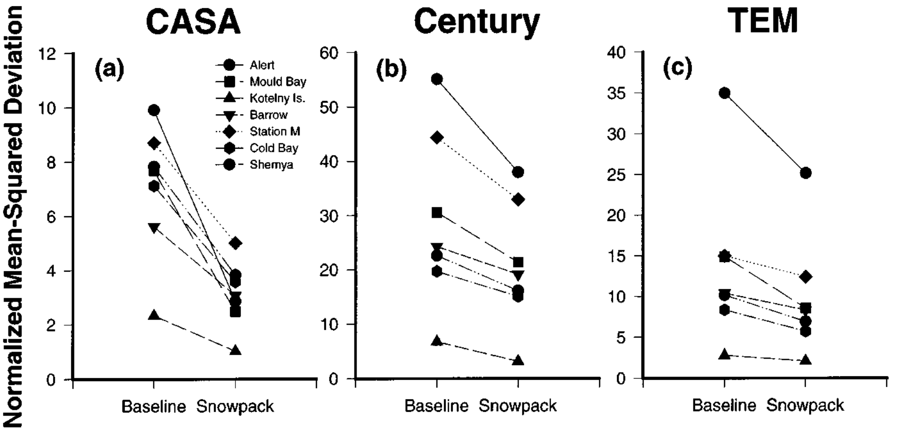

Figure 8. Comparison of the normalized mean-squared deviation between the baseline and snowpack simulations of the seasonal cycle of atmospheric CO_2 at the seven high latitude monitoring stations for (a) the Carnegie-Ames-Stanford Approach (CASA), (b) Century, and (c) the Terrestrial Ecosystem Model (TEM). The normalized mean-squared deviation (nmsd) is an index that indicates the degree of difference between the observed and simulated monthly concentrations of atmospheric CO_2 at a monitoring station, i.e., a nmsd of zero indicates no difference.

been recognized for decades (Kelley et al. 1968; Coyne & Kelley 1974). More recently, investigations by Oechel et al. (1997), Jones et al. (1999), and Grogan and Chapin (pers. comm.) have attempted to quantify heterotrophic respiration of tundra ecosystems during the nongrowing season. Oechel et al. (1997) used chambers to measure CO_2 exchange in wet sedge and tussock tundra in October, November, January, and May. From these measurements, Oechel et al. (1997) estimated releases of 20 g C m^{-2} from wet sedge tundra and 69 g C m^{-2} from tussock tundra between October and May. These estimates were spatially extrapolated by Oechel et al. (1997) to calculate the global release of CO_2 for wet sedge tundra (19 Tg C) and tussock tundra (60 Tg C) between October and May. In contrast to Oechel et al. (1997), Jones et al. (1999) used an IRGA connected to a stainless steel probe to measure CO_2 concentrations and applied a diffusion model to calculate the CO_2 release. From these measurements, Jones et al. (1999) estimated releases of at least 9.4 g C m^{-2} for coastal plain tundra and 8.4 g C m^{-2} for upland tussock between October and May. Grogan and Chapin (pers. comm.), who used a technique based on soda lime, estimated winter releases of 120 to 190 g C m^{-2} for three tussock tundra sites in Alaska. The releases of CO_2 from high latitude tundra between October and May estimated by the snowpack simulations of CASA (112 g C m^{-2}), Century (50 g C m^{-2}), and

TEM (62 g C m^{-2}) are within the range of measured CO_2 releases from tundra during the nongrowing season.

The variability among the estimates by Oechel et al. (1997), Jones et al. (1999), and Grogan and Chapin (pers. comm.) represents, in part, measurement error and spatial heterogeneity. Measurement error is one reason why the accuracy and precision of fluxes estimated by TBMs are difficult to evaluate with ground-based measurements. Spatial heterogeneity in fluxes across the landscape (Oechel et al. 1997; Jones et al. 1999) is another reason why additional variation in the observations will be unexplained by TBMs, which make estimates at much coarser spatial resolutions (0.5°) than the resolution of measurements (m^2 to hectares). Because of these two sources of variation, it is difficult for coarse-scale models to explain much more than 50% of the variation in observations that have not been used in model development or calibration (see Raich et al. 1991; Melillo et al. 1993; Kicklighter et al. 1994). Because of this limitation, it is difficult to evaluate the large-scale performance of TBMs with ground-based measurements, which are more effectively evaluated with site-specific modeling approaches (e.g., see Waelbroeck 1993; Waelbroeck & Louis 1995; Waelbroeck et al. 1997). Comparison of simulated CO_2 concentrations to observations at monitoring stations is one way to evaluate the large-scale seasonal dynamics of TBMs.

Although high latitude monitoring stations integrate seasonal CO_2 exchanges across much of the northern hemisphere, boreal forest and tundra tend to contribute more per unit area than temperate regions (see Kaminski et al. 1996). In addition, each of the high latitude stations is influenced by different regions within the northern hemisphere. For example, in comparison to other stations, the seasonal dynamics at Point Barrow are more enhanced by contributions from the Alaska peninsula and the dynamics at Shemya are influenced substantially by exchange in the eastern Asian continent (Kaminski et al. 1996). Because different high latitude stations integrate different regions of the globe, the simulation of atmospheric CO_2 provides a check on both the spatial and temporal qualities of CO_2 exchange by a TBM. The simulation of atmospheric CO_2 concentrations in this study indicates that the insulative effects of snowpack, as implemented in the TBMs in this study, improved the simulation of the seasonal dynamics of atmospheric CO_2 at high latitude monitoring stations during the late growing season and the nongrowing season.

Discrepancies between simulated and observed concentrations of atmospheric CO_2 in our simulations may, in part, be attributable to the ocean carbon cycle model and atmospheric transport model we used in this study. Because the seasonality of oceanic carbon exchange has little influence on northern hemisphere monitoring stations (Heimann et al. 1998), it is unlikely that discrepancies were caused by the HAMOCC3. In contrast, simulated CO_2 concentrations at high latitude stations may be sensitive to the simulation of atmospheric transport. There are a number of approaches to modeling atmospheric transport, and a recent intercomparison among global transport models (Law et al. 1996) revealed substantial differences in the concentration fields computed from the same prescribed surface sources by different transport models. The TM2 model in many respects performed close to the “typical” coarse grid transport model (Law et al. 1996). Differences between simulated and observed concentrations may, in part, be attributed to the extraction of CO_2 concentrations from a coarse grid transport model. Although it would be useful to assess the sensitivity of seasonal cycle simulations to transport models that operate at finer spatial resolutions, it is beyond the scope of our study.

Because we use potential vegetation to describe the land surface, our analyses do not fully consider carbon release associated with land-use nor carbon uptake associate with aforestation, nitrogen deposition, CO_2 fertilization, or other factors (see Schimel 1995). Although there are noticeable effects of tropical vegetation fires at certain tropical stations (Iacobellis et al. 1994; Wittenberg et al. 1998), there is little effect on simulations of the seasonal cycle at high latitude stations when fires in the boreal forest region are also considered (Wittenberg et al. 1998; McGuire, unpublished). Although net uptake of carbon in some regions is relevant to simulating the growth in the amplitude of atmospheric CO_2 that has been observed at some high latitude monitoring stations (Randerson et al. 1997), other issues are important to improving simulations of atmospheric CO_2 across all high latitude monitoring stations (Heimann et al. 1998).

A number of studies have used satellite-derived data from the Advanced Very High Resolution Radiometer (AVHRR) in modeling the seasonal signal of atmospheric CO_2 (Fung et al. 1987; Heimann & Keeling 1989; Knorr & Heimann 1995; Hunt et al. 1996; Randerson et al. 1996, 1997; Heimann et al. 1998; Sitch & McGuire, unpublished). In comparison to Century and TEM, the use of satellite-derived data is an important factor in the closer agreement between observed and estimated concentrations of atmospheric CO_2 for simulations using fluxes from CASA. Heimann et al. (1998) also observed that simulations using fluxes from the simple diagnostic biosphere model of Knorr and Heimann (1995), which uses satellite-derived data to define the phenology of NPP, fit the seasonal signal better in comparison to simulations that used fluxes from the five TBMs in the study that prognostically defined the phenology of NPP. In the BIOME3 model (Haxeltine & Prentice 1996), the use of satellite-derived phenology improves the timing of the beginning of the growing season to substantially improve simulation of the seasonal dynamics of atmospheric CO_2 at high latitude monitoring stations in comparison with phenology that is prognostically defined (Sitch and McGuire, unpublished). Although the simulation of Sitch and McGuire (unpublished) with satellite-derived phenology substantially improves the timing of the beginning of the growing season, it only partially improved estimates of CO_2 concentrations during the growing season and had no effect on CO_2 concentration during the nongrowing season. Our results are complementary to the simulations of Sitch and McGuire (unpublished), i.e., at high latitude monitoring stations the implementation of the snowpack formulation had: (1) little effect on the timing of the beginning of the growing season; (2) improved estimates of CO_2 concentrations during the late growing season, and (3) substantially improved the estimates of CO_2 concentrations during the nongrowing season.

In this study we have demonstrated that processes controlling the release of CO_2 from soils during the nongrowing season are relevant in the context of the global carbon cycle. This finding complements site-specific investigations of this issue (Kelley et al. 1968; Coyne & Kelley 1974; Waelbroeck 1993; Waelbroeck & Louis 1995; Waelbroeck et al. 1997; Oechel et al. 1997; Jones et al. 1999; Grogan & Chapin, pers. comm.). Although the implementation of the insulative effects of snowpack in this study allow us to simulate CO_2 concentrations at high latitude monitoring stations with more accuracy, it is important to recognize that the simple algorithm is a first-order approximation of the effects of snowpack on CO_2 release from cold season soils. A number of mechanisms may contribute to the release of CO_2 to the atmosphere from cold season soils. These include microbial activity at low temperature (Mazur 1980; Coxson & Parkinson 1987; Zimov et al. 1993, 1996; Brooks et al. 1995, 1996, 1997; Schimel & Clein 1996; Oechel et al. 1997), CO_2 release during phase changes from water to ice in freezing soil (Coyne & Kelley 1971; Oechel et al. 1997), freeze-thaw processes (Schimel & Clein 1996; Goulden et al. 1998), and spring thaw (Coyne & Kelley 1974; Kling et al. 1991; Goulden et al. 1998). Although we know that each of these processes may contribute to cold season release of CO_2 from soils, the relative contribution of these different mechanisms is not well understood (Jones et al. 1999). Studies that elucidate the relative importance of mechanisms controlling the release of CO_2 from snow-covered soils should be coupled with full-year measurements of CO_2 exchange using eddy covariance towers. Recently, year-round measurements of CO_2 exchange with tower technology have been made in tundra (Oechel and Vourlitis, unpublished) and boreal forest (Goulden et al. 1998). The capability to make year-round measurements of CO_2 exchange in snow-covered soils represents an important advance in the ability to develop and test the nongrowing season dynamics of process-based models. The understanding gained from simultaneous tower and process studies is essential for identifying which processes should be incorporated in global TBMs.

Acknowledgments

This research was supported by the Arctic System Science Program of the National Science Foundation (OPP-9614253), the Carbon Cycle Model Linkage Project of the Electric Power Research Institute (RP 3416-01), the Earth Observing System Program of the National Aeronautics and Space Administration (NAGW-2669), and the Taiga Long Term Ecological Research Program under funding from the National Science Foundation (DEB-9211769) and the USDA Forest Service (PNW 96-5024-2-CA).

References

Brooks PD, Williams MW, Walker DA & Smidt SK (1995) The Niwot Ridge snow fence experiment: Biogeochemical responses to changes in the seasonal snowpack. In: Tonnessen KA et al. (Eds) Biogeochemistry of Seasonally Snow-Covered Catchments (pp 293–301). International Association of Hydrological Cycles

Brooks PD, Williams MW & Smidt SK (1996) Microbial activity under alpine snowpacks, Niwot Ridge, Colorado. Biogeochemistry 32: 93–113

Brooks PD, Smidt SK & Williams MW (1997) Winter production of CO_2 and N_2O from alpine tundra: Environmental controls and relationship to inter-system C and N fluxes. Oecologia 110: 403–413

Beltrami H & Mareschal JC (1991) Recent warming in eastern Canada inferred from geothermal measurements. Geophysical Research Letters 18: 605–608

Chapin FS III, Shaver GR, Giblin AE, Nadelhoffer KJ & Laundre LA (1995) Responses of arctic tundra to experimental and observed changes in climate. Ecology 76: 694–711

Chapman WL & Walsh JE (1993) Recent variations of sea ice and air temperatures in high latitudes. Bulletin of the American Meteorological Society 74: 33–47

Conway TJ, Tans PP, Waterman LS, Thoning KW, Buanerkitzis DR, Masarie KA & Zhang N (1994a) Evidence for interannual variability of the carbon cycle from the NOAA/CMDL global air sampling network. J. Geophys. Res. 99D: 22,831–22,855

Conway TJ, Tans PP & Waterman LS (1994b) Atmospheric CO_2 from sites in the NOAA/CMDL air sampling network. In: Boden TA et al. (Eds) Trends ’93: A Compendium of Data on Global Change (pp 41–119) ORNL/CDIAC-65. Carbon Dioxide Information Analysis Center, Oak Ridge National Laboratory, Oak Ridge, TN, U.S.A.

Coxson DS & Parkinson D (1987) Winter respiratory activity in aspen woodland forest floor litter and soils. Soil Biol. Biochem. 19: 49–59

Coyne PI & Kelley JJ (1971) Release of carbon dioxide from frozen soil to the arctic atmosphere. Nature 234: 407–408

Coyne PI & Kelley JJ (1974) Variations in carbon dioxide across an arctic snowpack during spring. J. Geophys. Res. 79: 799–802

Cramer W, Kicklighter DW, Bondeau A, Moore B III, Churkina G, Nemry B, Ruimy A, Schloss A & the participants of “Potsdam ’95” (1999) Comparing global models of terrestrial net primary productivity (NPP): Overview and key results. Global Change Biology. In press

Field CB, Randerson JT & Malmstrom CM (1995) Ecosystem net primary production: Combining ecology and remote sensing. Remote Sens. Environ. 51: 74–88

Field CB, Berenfeld MJ, Randerson JT & Falkowski P (1998) Primary production of the biosphere: Integrating terrestrial and oceanic components. Science 281: 237–240

Fung I, Prentice K, Matthews E, Lerner J & Russel G (1983) Three-dimensional tracer model study of atmospheric CO_2: Response to seasonal exchanges with the terrestrial biosphere. J. Geophys. Res. 88C: 1281–1294

Fung IY, Tucker CJ & Prentice KC (1987) Application of advanced very high resolution radiometer vegetation index to study atmosphere-biosphere exchange of CO_2. J. Geophys. Res. 92D: 2999–3015

Goulden ML, Wofsy SC, Harden JW, Trumbore SE, Crill PM, Gower ST, Fries T, Daube BC, Fan S-M, Sutton DJ, Bazzaz A & Munger JW (1998) Sensitivity of boreal forest carbon balance to soil thaw. Science 279: 214–217

Haxeltine A & Prentice IC (1996) BIOME3: An equilibrium terrestrial biosphere model based on ecophysiological constraints, resource availability, and competition among plant functional types. Global Biogeochem. Cycles 10: 693–710

Heimann M (1995) The TM2 Tracer Model, Model Description and User Manual DKRZ Report 10, Max-Planck-Institute for Meteorology, Hamburg.

Heimann M & Keeling CD (1989) A three-dimensional model of atmospheric CO_2 transport based on observed winds: 2. Model description and simulated tracer experiments. In: Peterson DH (Ed) Aspects of Climate Variability in the Pacific and the Western Americas (pp 237–275). American Geophysical Union, Washington DC

Heimann M, Keeling CD & Tucker CJ (1989) A three dimensional model of atmospheric CO_2 transport based on observed winds: 3. Seasonal cycle and synoptic time scale variations. In: Aspects of Climate Variability in the Pacific and the Western Americas (pp 277–303). American Geophysical Union, Washington DC

Heimann M, Esser G, Haxeltine A, Kaduk J, Kicklighter DW, Knorr W, Kohlmaier GH, McGuire AD, Melillo JM, Moore B III, Otto RD, Prentice IC, Sauf W, Schloss A, Sitch S, Wittenberg U & Wurth G (1998) Evaluation of terrestrial carbon cycle models through simulations of the seasonal cycle of atmospheric CO_2: First results of a model intercomparison study. Global Biogeochem. Cycles 12: 1–24

Hunt ER, Piper SC, Nemani R, Keeling CD, Otto RD & Running SW (1996) Global net carbon exchange and intra-annual atmospheric CO_2 concentrations predicted by an ecosystem process model and three-dimensional atmospheric transport model. Global Biogeochem. Cycles 10: 431–456

Iacobellis SF, Frouin R, Razafimpanilo H, Somerville RCJ & Piper SC (1994) North African Savanna fires and atmospheric carbon dioxide. J. Geophys. Res. 99D: 8321–8334

Jones MH, Fahnestock JT & Welker JM (1999) Early and late winter CO_2 efflux from arctic tundra in the Kuparuk River watershed, Alaska. Arctic, Antarctic and Alpine Research. In press

Kaminski T, Giering R & Heimann M (1996) Sensitivity of the seasonal cycle of CO_2 at remote monitoring stations with respect to seasonal surface exchange fluxes determined with the adjoint of an atmospheric transport model. Physics of the Chemistry and the Earth 21: 457–462

Kelley JJ, Weaver DF & Smith BP (1968) The variation of carbon dioxide under the snow in the arctic. Ecology 49: 358–361

Kicklighter DW, Melillo JM, Peterjohn WT, Rastetter EB, McGuire AD, Steudler PA & Aber JD (1994) Aspects of spatial and temporal aggregation in estimating regional carbon dioxide fluxes from temperate forest soils. Journal of Geophysical Research 99D: 1303–1315

Kicklighter DW, Fischer A., Schloss AL, Plochl M, McGuire AD & the other participants of "Potsdam '95" (1999) Comparing global models of terrestrial net primary productivity (NPP): Global pattern and differentiation by major biomes. Global Change Biology. In press

Kling GW, Kipphut GW & Miller MC (1991) Arctic lakes and streams as gas conduits to the atmosphere: Implications for tundra carbon budgets. Science 251: 298–301

Knorr W & Heimann M (1995) Impact of drought stress and other factors on seasonal land biosphere CO_2 exchange studied through an atmospheric tracer transport model. Tellus 47B: 171–189

Lachenbruch AH & Marshall BV (1986) Climate change: Geothermal evidence from permafrost in the Alaskan arctic. Science 34: 689–696

Law RM, Rayner PJ, Denning AS, Erickson D, Fung IY, Heimann M, Piper SC, Ramonet M, Taguchi S, Taylor JA, Trudinger CM & Watterson IG (1996)Variations in modeled atmospheric transport of carbon dioxide and the consequences for CO_2 inversions. Global Biogeochem. Cycles 10: 783–796

Maier-Reimer E (1993) Geochemical cycles in an OGCM Part I: Preindustrial tracer distributions. Global Biogeochem. Cycles 7: 645–677

Marland G, Boden TA, Griffin RC, Huang SF, Kanciruk P & Nelson TR (1989) Estimates of CO_2 Emissions from Fossil Fuel Burning and Cement Manufacturing, Based on the U.S. Bureau of Mines Cement Manufacturing Data. ORNL/CDIAC-25, NDP-030, Carbon Dioxide Information Analysis Center, Oak Ridge National Laboratory, Oak Ridge, TN, U.S.A.

Mazur P (1980) Limits to life at low temperature and at reduced water contents and water activities. Origins of Life 10: 137–159

McGuire AD & Hobbie JE (1997) Global climate change and equilibrium responses of carbon storage in arctic and subarctic regions. In: Modeling the arctic system: A workshop report on the state of modeling in the Arctic System Science Program (pp 53–54). The Arctic Research Consortium of the United States, Fairbanks, AK, U.S.A.

McGuire AD, Melillo JM, Joyce LA, Kicklighter DW, Grace AL, Moore B III & Vörösmarty CJ (1992) Interactions between carbon and nitrogen dynamics in estimating net primary productivity for potential vegetation in North America. Global Biogeochem. Cycles 6: 101–124

McGuire AD, Melillo JM, Kicklighter DW & Joyce LA (1995) Equilibrium responses of soil carbon to climate change: Empirical and process-based estimates. J. Biogeography 22: 785–796

McGuire AD, Melillo JM, Kicklighter DW, Pan Y, Xiao X, Helfrich J, Moore B III, Vörösmarty CJ & Schloss AL (1997) Equilibrium responses of global net primary production and carbon storage to doubled atmospheric carbon dioxide: Sensitivity to changes in vegetation nitrogen concentration. Global Biogeochem. Cycles 11: 173–189

Melillo JM, McGuire AD, Kicklighter DW, Moore B III, Vörösmarty CJ & Schloss AL (1993) Global change and terrestrial net primary production. Nature 363: 234–240

Melillo JM, Kicklighter DW, McGuire AD, Peterjohn WT & Newkirk KM (1995) Global change and its effects on soil organic carbon stocks. In: Zepp RG & Sontagg Ch (Eds)

Role of Nonliving Organic Matter in the Earth's Carbon Cycle (pp 175–189). John Wiley & Sons

Nadelhoffer KJ, Giblin AE, Shaver GR & Linkins AE (1992). Microbial processes and plant nutrient availability in arctic soils. In: Chapin FS III et al. (Eds) Physiological Ecology of Arctic Plants: Implications for Climate Change (pp 281–300). Academic Press, New York

Oechel WC, Hastings SJ, Vourlitis GL, Jenkins MA, Reichers G & Grulke N (1993) Recent changes in arctic tundra ecosystems from a carbon sink to a source. Nature 361: 520–523

Oechel WC, Vourlitis GL, Hastings SJ & Bochkarev SA (1995) Change in arctic CO_2 flux over two decades: Effects of climate change at Barrow, Alaska. Ecological Applications 5: 846–855

Oechel WC, Vourlitis GL & Hastings SJ (1997) Cold season CO_2 emission from arctic soil. Global Biogeochem. Cycles 11: 163–172

Parton WJ, Schimel DS, Cole CV & Ojima DS (1987) Analysis of factors controlling soil organic matter levels in Great Plains grasslands. Soil Science Soc. Am. J. 51: 1173–1179

Parton WJ, Scurlock JMO, Ojima DS, Gilmanov TG, Scholes RJ, Schimel DS, Kirchner T, Menaut J-C, Seastedt T, Garcia Moya E, Kamnalrut A & Kinyamario JI (1993) Observations and modeling of biomass and soil organic matter dynamics for the grassland biome worldwide. Global Biogeochem. Cycles 7: 785–809

Raich JW & Potter CS (1995) Global patterns of carbon dioxide emissions from soils. Global Biogeochem. Cycles 9: 23–36

Raich JW, Rastetter EB, Melillo JM, Kicklighter DW, Steudler PA, Peterson BJ, Grace AL, Moore B III & Vörösmarty CJ (1991) Potential net primary productivity in South America: Application of a global model. Ecological Applications 1: 399–429

Randerson JT, Thompson MV, Malmstrom MV, Field CB & Fung IY (1996) Substrate limitation for heterotrophs: Implications for models that estimate the seasonal cycle of atmospheric CO_2. Global Biogeochem. Cycles 10: 585–602

Randerson JT, Thompson MV, Conway TJ, Fung IY & Field CB (1997) The contribution of terrestrial sources and sinks to trends in the seasonal cycle of atmospheric carbon dioxide. Global Biogeochem. Cycles 11: 535–560

Schimel DS (1995) Terrestrial ecosystems and the carbon cycle. Global Change Biology 1: 77–91

Schimel JP & Clein JS (1996) Microbial response to freeze-thaw cycles in tundra and taiga soils. Soil Biol. Biochem. 28: 1061–1066

Six KD & Maier-Reimer E (1995) Effects of plankton dynamics on seasonal carbon fluxes in an ocean general circulation model. Global Biogeochem. Cycles 10: 559–583

Thompson MV, Randerson JT, Malmstrom CM & Field CB (1996) Change in net primary production and heterotrophic respiration: How much is necessary to sustain the terrestrial carbon sink? Global Biogeochem. Cycles 10: 711–726

Tian H, Melillo JM, Kicklighter DW & McGuire AD (1999) The sensitivity of terrestrial carbon storage to historical atmospheric CO_2 and climate variability in the United States. Tellus. In press

Waelbroeck C (1993) Climate-soil processes in the presence of permafrost: A systems modelling approach. Ecological Modelling 69: 185–225

Waelbroeck C & Louis JF (1995) Sensitivity analysis of a model of CO_2 exchange in tundra ecosystems by the adjoint method. J. Geophys. Res. 100: 2801–2816

Waelbroeck C, Monfray P, Oechel WC, Hastings & Vourlitis G (1997) The impact of permafrost thawing on the carbon dynamics of tundra. Geophys. Res. Lett. 24: 229–232

Wittenberg U, Heimann M, Esser G, McGuire AD & Sauf W (1998) On the influence of biomass burning on the seasonal CO_2 signal as observed at monitoring stations. Global Biogeochem. Cycles 12: 531–544

Zimov SA, Zimova GM, Daviodov SP, Daviodova AI, Voropaev YV, Voropaeva ZV, Prosiannikov SF, Prosiannikova OV, Semiletova IV & Semiletov IP (1993) Winter biotic activity and production of CO_2 in Siberian soils: A factor in the greenhouse effect. J. Geophys. Res. 98: 5017–5023

Zimov SA, Davidov SP, Voropaev YV, Prosiannikov SF, Semiletov IP, Chapin MC & Chapin FS III (1996) Siberian CO_2 efflux in winter as a CO_2 source and cause of seasonality in atmospheric CO_2. Climatic Change 33: 111–120